Parametric Evaluation of the Performance Characteristics of Tightly Moored Wave Energy Converters for Several Floaters' Geometries

S.A. Mavrakos[1] and G.M. Katsaounis[2]

School of Naval Architecture and Marine Engineering,
National Technical University of Athens,
9, Heroon Polytechniou Ave., 157 73, Athens, Greece
[1]E-mail: mavrakos@naval.ntua.gr
[2]E-mail: katsage@mail.ntua.gr

Abstract

The paper investigates the effect that several floaters' geometries have on the performance characteristics of tightly moored vertical axisymmetric wave energy converters. A cylindrical buoy with and without vertical and horizontal skirts at its bottom, a cone along with two piston – like arrangements, consisting of an internal floater (cone or cylinder) and an exterior torus, have been examined and comparatively assessed. The WEC's first-order hydrodynamic characteristics are evaluated using a linearized diffraction – radiation semi-analytical method. Axisymmetric eigenfunction expansions of the velocity potential are introduced into properly defined ring – shaped fluid regions around the bodies and the potential solutions are matched at the boundaries of adjacent fluid regions by enforcing continuity of the hydrodynamic pressures and radial velocities.

A dynamical model for the floaters' performance in time domain is developed that properly accounts for the floaters hydrodynamic behaviour, the coupling terms between the different modes of motion and of the power take – off mechanism.

Numerical results showing parametrically the effect that the varying hydrodynamic characteristics of each particular floater's geometry have on the investigated WECs performance characteristics are presented and in terms of the expected power production discussed.

Keywords: Converter, Ocean wave energy, Point absorber, WEC.

1 Introduction

Ocean wave energy conversion by exploiting the interaction of single or multiple floating bodies with sea waves has been the subject of many research efforts during the last decades. The problem of maximizing the captured energy has been attacked either by suitably choosing the hydrodynamic and mechanical characteristics of the devices to achieve resonant motion, or by applying specific control strategies, in order to properly guide the motion of the float. The work presented herein is focused on the first approach. We examine the influence of the float shape on the power conversion, for small size devices operating in shallow water depths.

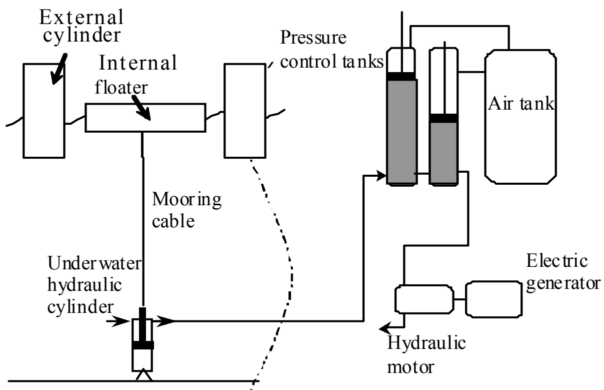

Figure 1: Operation principle for the WEC system

The operational principle of the WECs under consideration is in many aspects, typical of the devices of the kind [1-4]. The converter is assumed to operate in shallow water. It is composed by an internal floater, tight moored to the sea bottom. The mooring cable is connected to the piston of an underwater hydraulic cylinder. The moving floater is surrounded by an external concentric cylinder. The incoming sea waves enforce the cylinders to perform oscillations along their five degrees of freedom, the sixth degree (i.e. rotation about the vertical axis) being not considered, due to the axisymmetric shape of the device. The vertical motion of the internal floater activates the piston of the underwater main hydraulic cylinder.

During the upward motion, the cylinder feeds with pressurized fluid the pressure control tanks of the device, which are supported by an air tank of sufficient volume. This permits the discharge of the pressurized fluid to the hydraulic generator of the system at constant pressures. The vacuum generated in the opposite volume of the hydraulic cylinder (or a similar force generated by suitable mechanical system) serves as restoring force, giving at the same time a pretension to the buoy system.

Non-return valves are included in the system to ensure the proper circulation of the hydraulic fluid. At the present stage a low pressure open system is considered, working with sea water, which is entering into the system in the underwater cylinder and is being discharged after the hydraulic generator.

When considering tight moored configurations the hydraulic piston is assumed connected to the internal cylinder, as shown in figure 1. For the unrestricted case of motion of the two bodies (figure 2) the hydraulic piston is assumed to act between the two floating bodies, exploiting the difference of their motions in heave.

2 Dynamic Formulation

The equation of the dynamic equilibrium of the cylinders in the five degrees of freedom considered (i.e. surge, sway, heave, roll and pitch), can be obtained using inertial and body fixed reference systems (Fig.2a and b). Although the paper is focused on tight moored configurations and the numerical results that will be presented later correspond to floater with sideway restrictions, the developed theoretical model presented herein includes all the degrees of motion.

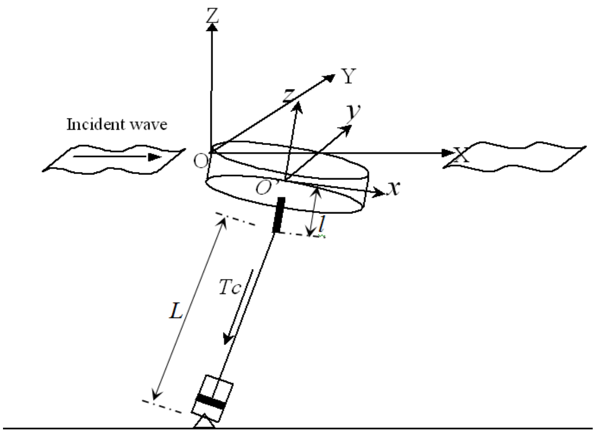

Figure 2a: Reference configurations for dynamic equilibrium (single body)

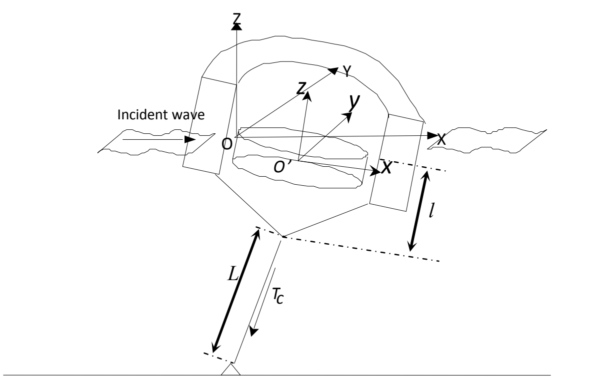

Figure 2b: Reference configurations for dynamic equilibrium (double body configuration)

The origin O of the inertial system O-XYZ is fixed at the intersection between the still sea level and the vertical symmetry axis of the cylinders in their rest position, the z-axis being pointing upwards. Body attached systems, O'-xyz and O''-xyz, with their origins located at the center of the gravity of the internal (body 1) and external cylinder (body 2) respectively, are used for the description of the motions of the bodies. The z-axes of the systems coincide in the rest position, while their x- and y- axes are parallel.

Denoting by ξ the degrees of freedom of the system, with $\xi_1 \sim \xi_3$ being the translational components of the displacements of the body 1 relative to the axes of the inertial system, ξ_4 and ξ_5 the corresponding rotational angles around the axes OX and OY of the same body, $\xi_6 \sim \xi_8$ the translational components for the external body and ξ_9, ξ_{10} the corresponding rotational ones, the dynamic equilibrium gives :

$$[m_s]\ddot{\vec{\xi}}(t) + [K]\,\vec{\xi}(t) = \vec{F}_H(t) + \vec{F}_c(t) + B_1\vec{k} - m_1 g\,\vec{k} + B_2\vec{k} - m_2 g\,\vec{k} \tag{1}$$

where:

$\vec{\xi}(t)$ is the generalized vector of the displacements including both translational and rotational components of the two bodies. For the case of a tight moored configuration only the ξ_3 displacement is considered.

$[m_s]$ is the inertia matrix including any structural mass and, possibly, ballast. Denoting by m the mass and assuming that the floater-attached co-ordinate systems coincide with the principal inertial axes of the bodies, then matrix m_s is given by:

$$[m_S] = diag[m_1, m_1, m_1, I_{1xx}, I_{1yy}, m_2, m_2, m_2, I_{2xx}, I_{2yy}] \tag{2}$$

$[K]$ is the hydrostatic stiffness matrix. Denoting by Δ the displacement, A_{WL} the waterplane area and GM the metacentric height, the K matrix takes the form:

$$[K] = diag[0, 0, \rho g A_{WL1}, \Delta_1 GM_1, \Delta_1 GM_1, 0, 0, \rho g A_{WL2}, \Delta_2 GM_2, \Delta_2 GM_2] \tag{3}$$

$B_i\vec{k}$ is the net buoyancy of the body i, directed upwards, $\vec{k}$ being the unit vector along the OZ axis.

$m_i g\vec{k}$ is the weight of the body i.

$\vec{F}_H(t)$ is the vector of the hydrodynamic loads exerted on the bodies, including both diffraction and radiation components.

$\vec{F}_C(t)$ is the vector of the forces and moments due to the tension of the mooring cable. Considering the geometries of both the floater and the cable and assuming small (linearized) displacements and rotations, it can be obtained, for the single body configuration (fig. 2a), that:

$$\vec{F}_C = \begin{bmatrix} -T_C\left(\xi_1 - l\xi_5\right)/L \\ -T_C\left(\xi_2 + l\xi_4\right)/L \\ -T_C \\ -T_C l(\xi_2 + l\xi_4)/L \\ T_C l(\xi_1 - l\xi_5)/L \end{bmatrix} \tag{4}$$

where T_c is the time depended tension (including any pretension) along the mooring cable, l is the length measured from the center of the floater to the latching point and L is the distance from the latching point to the sea bottom. For the double body configuration the degrees of freedom ξ_i, i=1~5 in (4) above should be replaced by the corresponding degrees of the outer torus ξ_i, i=6~10.

The hydrodynamic forces up to first-order that are exerted on the bodies along the k direction can be analyzed in the time-domain using the impulse response function method, as follows [5]:

$$F_{H,k}(t) = -\sum_{j=1}^{10}\left\{\bar{a}_{kj}.\ddot{\xi}_j(t) + \int_{-\infty}^{t} R_{kj}(t-\tau).\dot{\xi}_j(\tau)d\tau\right\} + F_{D,k}(t) + F_{w,k}(t) \tag{5}$$

where $\bar{a}_{kj}$ is the frequency independent hydrodynamic added mass coefficient (force / moment exerted along the d.o.f k due to a unit acceleration along the d.o.f. j) and corresponds to the limit of the hydrodynamic mass coefficient when the frequency tends to infinity, i.e. $\bar{a}_{kj} = \lim_{\omega\to\infty} a_{kj}(\omega)$. It holds:

$$\bar{a}_{kj} = a_{kj}(\omega) + \frac{1}{\omega}\int_0^\infty R_{kj}(\tau)\sin(\omega t)d\tau \tag{6}$$

$R_{kj}(t)$: is the kj element of the hydrodynamic retardation matrix, giving the time history of the force / moment exerted along the d.o.f k due to a unit velocity impulse along the d.o.f j at time t = 0. Based on the frequency - dependent hydrodynamic damping coefficients, the retardation functions are given by:

$$R_{kj}(t) = \frac{2}{\pi}\int_0^\infty b_{kj}(\omega)\cos(\omega t)d\omega \tag{7}$$

$F_{D,k}(t)$: is the drag force in the k direction, (k =1~3 for the first body or 6~8 for the second body), expressed by the equation:

$$F_{D,k}(t) = \frac{1}{2}C_{iD}A_{iw}\rho\ \left(w_{kp}(t) - \dot{\xi}_k(t)\right)\left| w_{kp}(t) - \dot{\xi}_k(t)\right| \tag{8}$$

where C_{iD} is the drag coefficient of the body i in the k direction, w_{kp} is the wave particle velocity and ρ is the density of the water. Although the drag forces, $F_{D,k}(t)$, can be of minor importance for the floater's motion, they are incorporated in the formulation of the problem for the sake of completeness.

$F_{w,k}(t)$ is the time realization of the first-order wave exciting force on the bodies in the k direction, in a given sea state. It is given by:

$$F_{w,k}(t) = \left(\frac{F_{w,k}(\omega,\theta)}{A}\right)\cdot A\cdot\cos\left[\omega t + \phi_k(\omega)\right] \tag{9}$$

in the case of an incident monochromatic wave with a wave height of $2A$, angle of attack θ and cyclic frequency ω and by

$$F_{w,k}(t) = \sum_{i=1}^{N}\sum_{l=1}^{M}\left(\frac{F_{w,k}(\omega_i,\theta_l)}{A}\right)\sqrt{2S(\omega_i,\theta_l)\Delta\omega\Delta\theta}\ x \\ \cos\left(\omega_i t + k_i x\cos\theta_l + k_i y\sin\theta_l + \phi_k\left(\omega_i,\theta_l\right) + \varepsilon_{il}\right) \tag{10}$$

in the case of incident short-crested irregular waves [6]. N and M are the numbers of wave frequencies and wave directions resolved in the wave energy spectrum.

Moreover, $\left(F_{w,k}(\omega_i,\theta_l)/A\right)$ is the frequency-dependent wave exciting force transfer function per unit wave amplitude exerted along the k d.o.f. The spectral density $S(\omega_i, \theta_l)$ is found from the directional spectrum and the choice of the frequency band $\Delta\omega$ determines some characteristics associated with generation of irregular waves, e.g. repetition of the irregular wave train. ε_{il} and φ_k are random phase angles of wave component number il that are uniformly distributed in [0, 2π] and the phase-lag associated with the exciting wave load on the floater in k direction, respectively.

The first- order wave load, $\left(F_{w,k}(\omega_i,\theta_l)/A\right)$, is evaluated through the integration of the first-order hydrodynamic pressure due to the incident, φ_I, and the diffracted, φ_d, wave fields on the mean wetted surface, S, of the cylindrical buoy. It holds:

$$F_{w,k} = i\omega\rho\iint_S\left(\varphi_I + \varphi_d\right)n_k dS \tag{11}$$

In the framework of the present paper, the frequency-dependent first- order wave exciting loads on the floater and the corresponding phase angles due to a wave of unit amplitude are obtained by solving the wave diffraction problem for any given floaters' geometry using an exact method within the framework of the potential flow theory. An outline of the method will be presented in the next section.

The expression of the vertical tension of the cable $T_c(t)$ is derived from the consideration of the equilibrium of the piston of the hydraulic cylinder and the operation of the pressure control tanks.

For simplicity in the formulation and due to the fact that the water depth is considered small, the short mooring cable of the floater is assumed massless and inextensible. Furthermore, a small downward restoring force is also assumed acting on the cable, just to prevent it from being slack. This force is due to either the vacuum generated in the opposite volume of the piston during the upward motion of the cylinder or it is due to suitable restoring springs. In this way, the piston rod and the inner floater have the same vertical velocity, according to the linearized model used in the Eqs. (4), and the condition for the determination of the force in suction phase is determined by the following equation:

$$T_C = T_{pre} \qquad for\ \dot{\xi}_3 < \varepsilon$$
$$or \tag{12}$$
$$T_C = T_{pre} + p_p A_p \quad for\ \dot{\xi}_3 \geq \varepsilon$$

where T_{pre} is the pretension in the cable assumed constant for simplicity, p_p is the temporal compression pressure and A_p is the corresponding piston area. The compression phase is determined by the value of the vertical velocity $\dot{\xi}_3(t)$. When this velocity is positive (or greater than a small quantity ε, for the stability of the numerical implementation) a non return valve is activated and permits the compression of the fluid from the cylinder to the pressure tanks, at a volumetric flow rate of:

$$Q = A_p \dot{\xi}_3(t), \qquad \dot{\xi}_3(t) \geq \varepsilon \tag{13a}$$

The entrance of the pressurized fluid into the tanks through an orifice of area A_o and coefficient μ results in a pressure drop [4] of:

$$\Delta p = \frac{\rho}{2\mu^2 A_0^2} Q^2 \tag{13b}$$

Thus, the pressure in the hydraulic cylinder during the compression phase is related to the pressure p_0 in the tanks by the relation:

$$p_p = \Delta p + p_0 = \frac{\rho}{2\mu^2 A_0^2} Q^2 + p_0 \tag{13c}$$

Pressure p_0 is assumed constant, maintained by an air tank of sufficient volume. Relations (13a-c) can be combined to (12) in order to express T_C as a function of the vertical velocity $\dot{\xi}_3(t)$.

The produced mechanical power is evaluated from the fluid flow by the relation:

$$P(t) = Q(t)\ p_0 \tag{13d}$$

The useful energy produced can be estimated by a simplified model of the power generator:

$$P_u(t) = \eta\ P(t) \tag{13e}$$

where η is the efficiency of the generator.

Due to the fact that the velocities of the bodies (both translational and angular) are unknown at the current time t, i.e. $\dot{\xi}(t)$, a problem in the numerical implementation of the Eq. (5) arises, that is associated with the evaluation of the integral:

$$I = \int_{-\infty}^{t} R_{kj}(t-\tau)\dot{\xi}_j(\tau)d\tau\ , \tag{14}$$

In order to tackle the difficulty, the Newmark's method for the numerical integration of the equations of motion has been used [7]. Following this method, by assuming that the solution of the problem (i.e.: $\xi_k, \dot{\xi}_k, \ddot{\xi}_k$), is known at discrete time instances t-Δt, t-$2\Delta t$, t-$3\Delta t$… prior to the current time t, we substitute the unknown velocities and accelerations for the current time, by the formulae:

$$\ddot{\xi}(t) = b_1(\xi(t) - \xi(t-\Delta t)) + b_2\dot{\xi}(t-\Delta t) + b_3\ddot{\xi}(t-\Delta t)$$
$$\dot{\xi}(t) = b_4(\xi(t) - \xi(t-\Delta t)) + b_5\dot{\xi}(t-\Delta t) + b_6\ddot{\xi}(t-\Delta t) \tag{15}$$

where the constants b_1 to b_6 depend on the specific variant of the Newmark method used and the time step increment Δt. In this way, the integral 'I ', Eq. (14), can be evaluated using the trapezoidal integration:

$$I = \sum_{n=1}^{N}\left\{R_{kj}(n\Delta t)\dot{\xi}_k(t-n\Delta t)\ \Delta t\right\} + \tfrac{1}{2} R_{kj}(0)\dot{\xi}_k(t)\Delta t \tag{16}$$

By substituting the expression for the velocity $\dot{\xi}_k(t)$ given previously, in Eq. (15), a form can be obtained that depends only on known quantities and on the basic unknown vector $\xi(t)$. This expression can then be introduced in Eq. (5), in order to solve Eq. (1) for the unknown displacements $\xi(t)$ at the current time step. It is evident that past information on $\dot{\xi}(t)$ are entered in (14). For the numerical implementation, an appropriate length of the time-memory window, which is determined by the value of N in (14) above, should be selected, in order to include all the variations of the retardation functions, (see for example Figure 8).

For the a piston-like arrangement the internal body is assumed moving inside the outer cylinder like a piston, guided by suitable rollers, fixed on the outer body. For this case the equation of the dynamic equilibrium (1) has to be supplemented by the displacement compatibility relations, which describe the constraints imposed on the inner body, to act like a piston, inside the outer cylinder. Up to linear terms this condition is expressed by the following constraints:

$$\xi_1 = \xi_6,\ \xi_2 = \xi_7,\ \xi_4 = \xi_9,\ \xi_5 = \xi_{10} \tag{16a}$$

The model described by the Eqs. (1) to (13) is highly non linear, mainly due to the expression for the cable tension (Eq. 12) and merely due to the expression for the pressure drop (Eq. 13b). Due to these nonlinearities a numerical solution scheme in the time domain is required. In conjunction with the Newmark scheme for the time integration, mentioned previously, an iterative solution based on the Newton Raphson method was implemented in the algorithm, to handle the nonlinearities.

3 Hydrodynamic Formulation

We consider two concentric, free – surface piercing truncated cylinders with vertical symmetry axes that are exposed to the action of regular waves with amplitude (H/2) and frequency ω in constant water depth h (Figures 2 and 3).

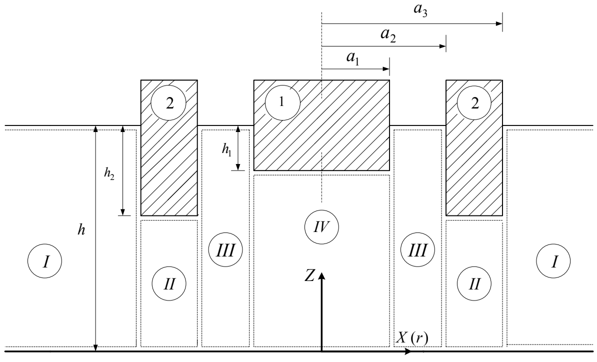

Figure 3: Main dimensions and fluid regions for the piston-like arrangement

Cylindrical coordinates (r, θ, z) are introduced with origin at the still water plane with its vertical axis Oz directed upwards. Assuming that the flow is irrotational and inviscid and that the waves are of small slope, classical linearized water wave theory can be employed. The fluid flow can be described by the potential function:

$$\Phi(r,\vartheta,z;t) = \mathrm{Re}\left[\varphi(r,\vartheta,z)e^{-i\omega t}\right] \tag{17}$$

With

$$\varphi(r,\vartheta,z) = \varphi_0(r,\vartheta,z) + \varphi_7(r,\vartheta,z) + \sum_{p=1}^{2}\sum_{j=1}^{5}\dot{\xi}_{j0}^{(p)}\varphi_j^{(p)}(r,\vartheta,z) \tag{18}$$

Here, φ_0 is the velocity potential of the undisturbed incident harmonic wave, φ_7 is the diffraction potential for the bodies fixed in the wave field and $\varphi_j^{(p)}$ (j = 1, 2, 3, 4, 5; p = 1, 2) are the radiation potentials resulting from the forced motion of body p in the j-th d.o.f with unit velocity amplitude $\dot{\xi}_{j0}^{(p)}$. The diffraction wave field around the fixed bodies is described by the potential:

$$\varphi_D(r,\vartheta,z) = \varphi_0(r,\vartheta,z) + \varphi_7(r,\vartheta,z) \tag{19}$$

The undisturbed incident wave train, φ_0, propagating at an angle β with respect to the positive x-axis can be expressed in the cylindrical co-ordinate frame of the body as follows:

$$\varphi_0(r,\vartheta,z) = -i\omega\left(\frac{H}{2}\right)\sum_{m=-\infty}^{\infty} i^m \Psi_{0,m}(r,z)e^{im\vartheta} \tag{20}$$

with:

$$\frac{1}{h}\Psi_{0,m}(r,z) = \frac{Z_0(z)}{h\,Z_0'(0)}J_m(kr)e^{-im\beta} \tag{21}$$

Here, J_m is the m-th order Bessel function of the first kind and $Z_0(z)$ is defined by:

$$Z_0(z) = \left[\frac{1}{2}\left[1+\frac{\sinh(2kh)}{2kh}\right]\right]^{-1/2}\cosh\left[k(z+h)\right] \tag{22}$$

and $Z'_0(0)$ is its derivative at z = 0. Frequency ω and wave number k are related by the dispersion equation:

$$\omega^2 = gk\tanh(kh) \tag{23}$$

In accordance to Equation (20) the total diffracted potential (including the incident field) of the flow field around the restrained structures can be written in the form:

$$\varphi_D(r,\vartheta,z) = -i\omega\left(\frac{H}{2}\right)\sum_{m=-\infty}^{\infty} i^m \Psi_{Dm}(r,z)e^{im\vartheta} \tag{24}$$

The fluid flow caused by the forced oscillation of the bodies in otherwise still water is symmetric about the $\vartheta = 0^0$ - plane and antisymmetric about the $\vartheta = \pi/2$ - plane for surge, (j = 1), and pitch, (j = 5), whereas it is symmetric about both these planes for heave, (j = 3). Thus the corresponding velocity potentials for these modes of motion can be expressed as, p = 1, 2:

$$\varphi_1^{(p)}(r,\vartheta,z) = \Psi_{11}^{(p)}(r,z)\cos\vartheta \tag{25}$$

$$\varphi_3^{(p)}(r,\vartheta,z) = \Psi_{30}^{(p)}(r,z) \tag{26}$$

$$\varphi_5^{(p)}(r,\vartheta,z) = \Psi_{51}^{(p)}(r,z)\cos\vartheta \tag{27}$$

The complex functions Ψ_{Dm}, $\Psi_{11}^{(p)}$, $\Psi_{30}^{(p)}$ and $\Psi_{51}^{(p)}$ in Eqs. (24) – (27) are the principal unknowns of the problem. The potentials $\varphi_j^{(p)}$ (j = 1, 2, 3, 4, 5; p = 1, 2) and φ_7 must satisfy the Laplace equation in the entire fluid domain, the zero normal velocity on the sea bed, z = -h, and the free-surface condition on the mean water surface, z = 0. Furthermore, $\varphi_j^{(p)}$ has to fulfill following kinematic conditions on the mean bodies wetted surface $S^{(q)}_0$:

$$\frac{\partial\varphi_D}{\partial\mathbf{n}^{(q)}} = 0 \; and \; \frac{\partial\varphi_j^{(p)}}{\partial\mathbf{n}^{(q)}} = \delta_{pq}n_j^{(p)}, j=1...5; p,q=1,2 \tag{28}$$

where $\partial(\;)/\partial\mathbf{n}^{(q)}$ denotes the derivative in the direction of the outward unit normal vector $\mathbf{n}^{(q)}$ to the mean wetted surface $S^{(q)}_0$ of the body q and $n^{(p)}_j$ are its generalized components defined as $(n^{(p)}_1, n^{(p)}_2, n^{(p)}_3) = \mathbf{n}^{(p)}$ and $(n^{(p)}_4, n^{(p)}_5, n^{(p)}_6) = \mathbf{r} \times \mathbf{n}^{(p)}$ where $\mathbf{r}$ is the position vector with respect to the origin of the coordinate system of body p. Finally, a radiation condition must be imposed which states that propagating disturbances must be outgoing.

The unknown functions Ψ_{Dm}, $\Psi_{11}^{(p)}$, $\Psi_{30}^{(p)}$ and $\Psi_{51}^{(p)}$ in Eqs. (24) – (27) can be obtained using matched axisymmetric eigenfunction expansions [8-13]. Here, by the way of example, the series representation of the above functions, in the external fluid region I, see Fig. 3, are given:

$$\frac{1}{\delta_j}\Psi_{jm}^{I,(p)}(r,z) = f_{jm}^{I,(p)}(r,z) + \sum_{l=0}^{\infty}F_{j,ml}^{I,(p)}\frac{K_m(\alpha_l r)}{K_m(\alpha_l a_3)}Z_l(z), p=1,2 \tag{29}$$

where:

$$f_{Dm}^{I,(p)}(r,z) = J_m(kr).e^{-im\beta}\frac{Z_0(z)}{h.Z_0'(0)}$$

$$f_{11}^{I,(p)}(r,z) = f_{30}^{I,(p)}(r,z) = f_{51}^{I,(p)}(r,z) = 0 \tag{29a}$$

$$\delta_D = \delta_1 = \delta_2 = \delta_3 = h,\; \delta_4 = \delta_5 = h^2$$

The first term in the above equation represents the contribution of the undisturbed incident wave to the total wave potential around the bodies. Moreover, K_m are the m-th order modified Bessel function of second kind, whereas $Z_j(z)$ are orthonormal functions in [-h, 0] defined by:

$$Z_j(z) = \left\{\frac{1}{2}\left[1+\frac{\sin(2\alpha_j h)}{2\alpha_j h}\right]\right\}^{-1/2}\cos\left[\alpha_j(z+h)\right] \tag{29b}$$

The eigenvalues α_j are roots of the transcendental equation

$$\frac{\omega^2}{g} + \alpha_j\tan(\alpha_j h) = 0 \tag{29c}$$

with α_0 = -ik being purely imaginary

4 Examined Floaters

Initially two groups of floaters have been examined, corresponding to displacements of 12.57 and 42.41 m^3, respectively. The dimensions of the bodies in each group are shown in Figure 4 and Tables 1 and 2.

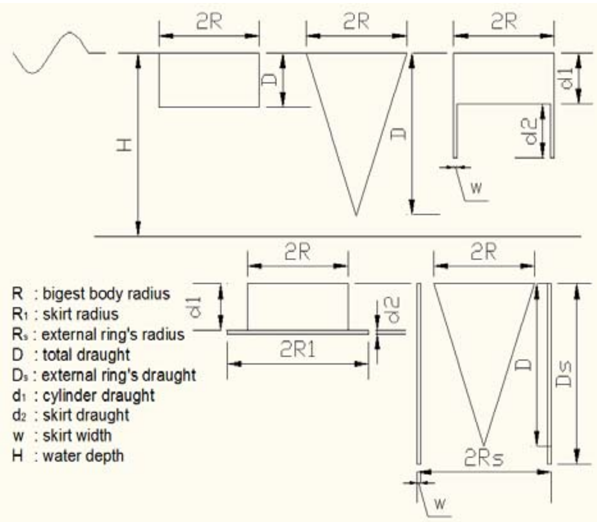

Figure 4: Definition of Geometry

No	Float geometry	R	R_1	R_s	D	D_s	d_1	d_2	w	H
1	Cylinder	2	-	-	1	-	-	-	-	10
2	Cone	2	-	-	3	-	-	-	-	10
3	Cylinder Skirt	2	2	-	1.9	-	0.9	1	0.1	10
4	Compound Cylind	2	2.83	-	0.9	-	0.8	0.1	-	10
5	Cone Ring	2	-	3	3	3.5	-	-	0.1	10

Table 1: Float Dimensions (m). Displacement V = 12.57 m^3

No	Float geometry	R	R_1	R_s	D	D_s	d_1	d_2	w	H
1	Cylinder	3	-	-	1.5	-	-	-	-	10
2	Cone	3	-	-	4.5	-	-	-	-	10
3	Cylinder Skirt	3	3	-	2.9	-	1.4	1.5	0.1	10
4	Compound Cylinder	3	4.24	-	1.4	-	1.3	0.1	-	10
5	Cone Ring	3	-	4	4.5	5	-	-	0.1	10

Table 2: Float Dimensions (m). Displacement V = 42.41m^3

The hydrodynamic formulation of the previous chapter was applied and representative results for the frequency dependent added masses, hydrodynamic damping and diffraction forces are shown in figures 5-7, for the case of V=12.57 m^3. For the first three bodies considered (cylinder, cone, cylinder with vertical skirt) smooth variations of the hydrodynamic parameters can be observed in the graphs. The compound cylinder displays a zero value of the damping and diffraction coefficients, which is characteristic for such bodies and corresponds to the well known cancellation frequency.

An even more peculiar behavior is observed in the results of the cone-ring combination. Here a piston-like heave motion of the internal cone is assumed, while the external torus remains steady. Abrupt variations of the hydrodynamic parameters are observed in the vicinity of 1.75 rads/sec, which corresponds to the resonance of the confined fluid in the annular area between the internal, piston – like cone and the exterior toroidal body. For the lower frequency range these parameters take, in general, higher values, as compared to the other bodies.

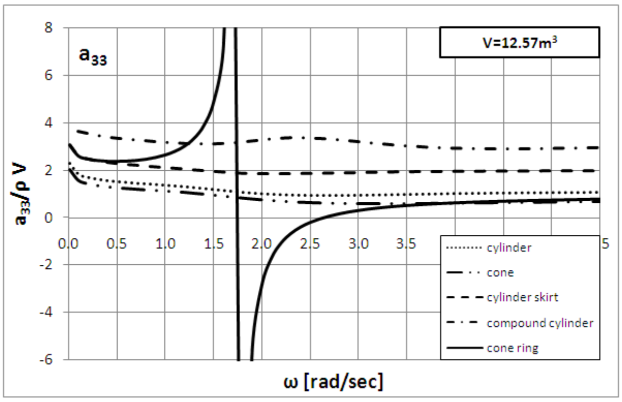

Figure 5: Hydrodynamic mass coefficients in heave motion. V=12.57m^3

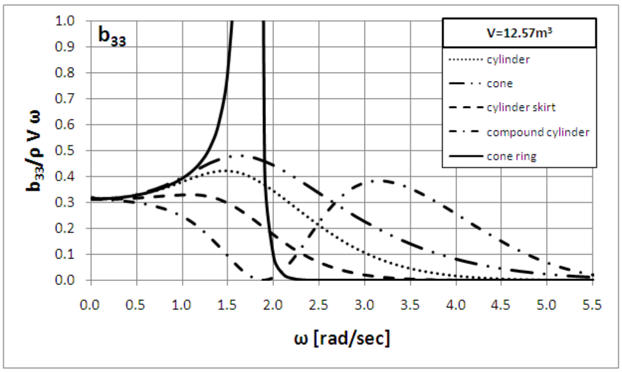

Figure 6: Damping coefficients in heave motion. V=12.57m^3

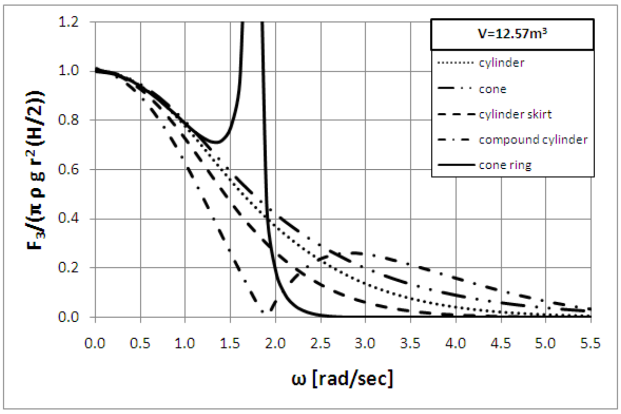

Figure 7: Wave exciting forces in heave direction. V=12.57m^3

Figure 8 presents the time histories of the retardation functions for heave motion. Again, the distinguished behavior of the cone-ring combination is evident, exhibiting strong oscillations at a frequency corresponding to the observed peak in the hydrodynamic parameter graphs.

In order to investigate further the behavior of point absorbers consisting of two concentric axisymmetric bodies, a second piston-like arrangement was studied, consisting of an internal cylinder and an external torus (Figure 9). The dimensions of this configuration, which corresponds to a displaced volume of 117.8m^3 for the internal body, are also displayed in the same figure. The hydrodynamic performance of this arrangement was thoroughly examined in [12] where the same peculiar behavior, like the cone-ring arrangement, was observed in the values of the hydrodynamic parameters. As an example, figures 10 and 11 show a comparison of the diffraction forces and the hydrodynamic damping parameter in heave, for the internal cylinder, with and w/o the external torus.

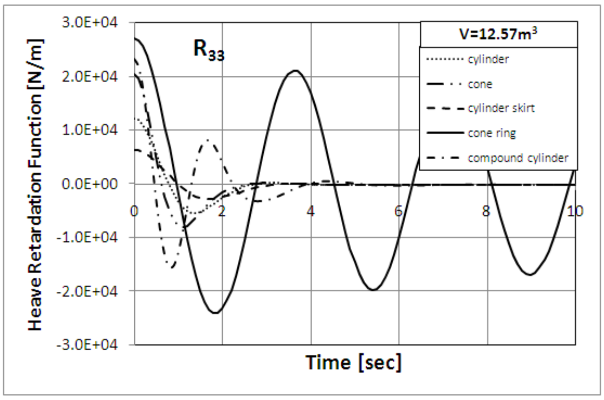

Figure 8: Retardation functions for heave motion. V=12.57m^3

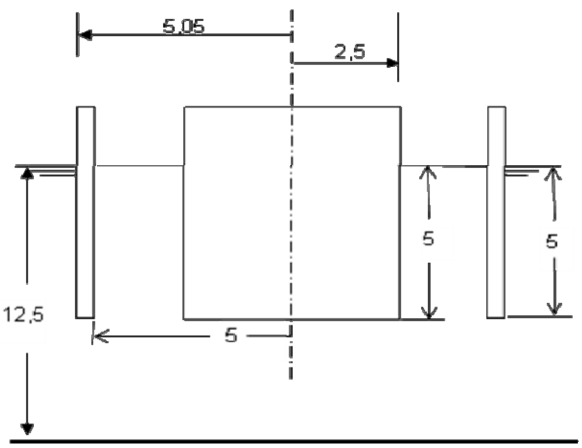

Figure 9: Two cylinder piston-like arrangement. Dimensions (m)

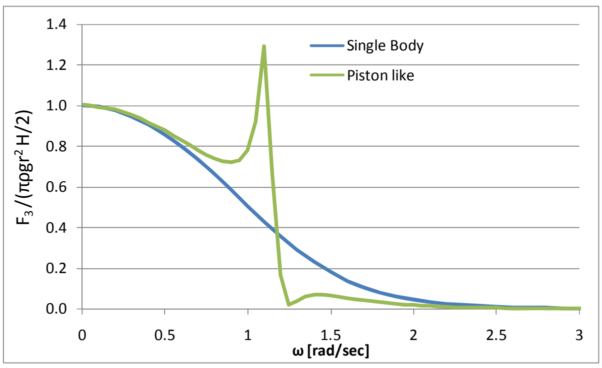

Figure 10: Internal cylinder, diffraction force in heave

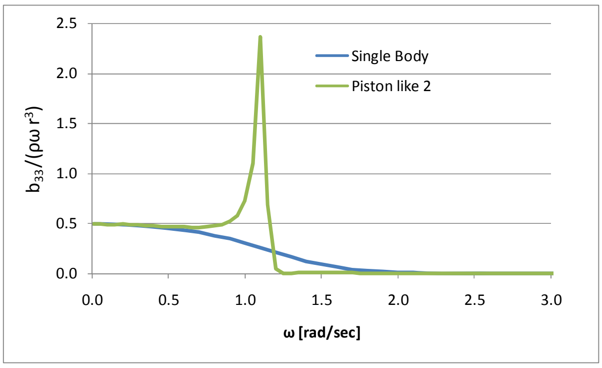

Figure 11: Internal cylinder, hydrodynamic damping

5 Power Absorption

Time simulations of the floaters' motion were performed, applying the developed numerical model. Bretschneider wave spectra were assumed for the incoming waves and sea states in the range of H_s=0.5~1.3 and T_e=2.25~5.38 were examined. The time step used in the simulations was 0.1 sec, while the total simulation length was 20 minutes. The floaters were assumed to be restricted to the side way motions and rotations, corresponding to a tightly moored configuration. The power take off mechanism was introduced to the model as a linear damper, for the purposes of comparisons. The pertinent damping value was properly selected in order to maximize the absorbed energy for each case.

The efficiency of each configuration was measured as the fraction of the absorbed power over the wave power incoming to the diameter of each body. Tables 3 and 4 show the efficiency values for each examined case.

Sea State		**Floater**				
H_s (m)	T_e (sec)	Cylinder	Cone	Cylinder skirt	Comp. cylinder	Cone-ring
0.5	2.70	31	33	25	5	18
	3.16	32	34	30	12	36
	3.85	28	30	27	15	42
0.7	3.16	32	34	30	13	38
	3.85	28	30	28	15	41
	4.14	28	31	27	17	42
0.9	3.85	29	30	28	15	41
	4.14	29	31	26	18	43
	4.90	26	25	24	16	36
1.1	4.14	29	30	27	17	42
	4.90	26	27	24	16	37
1.3	4.90	25	26	25	17	36
	5.38	23	25	22	17	32

Table 3: Efficiency (%)-Displacement V=12.57m^3

A resembling behavior is observed among the results of the cylinder, the cone and the cylinder with the vertical skirt. On the other hand, the results for the compound cylinder display lower values for all the examined cases. This fact can be explained by the lower values and zeroings that the hydrodynamic damping and wave diffraction exhibit in the examined frequency ranges (see figures 6 and 7).

Examining the low displacement case (Table 3), it can be concluded that the cone-ring combination absorbs more power for the majority of the examined sea states. However, considering the higher displacement (Table 4), the above result remains true only for the upper limit of the examined periods, where this floater exhibits the maximum performance of all the cases considered. For the rest of the frequency range, the efficiency takes significantly lower values.

Sea State		Floater				
H_s (m)	T_e (sec)	Cylinder	Cone	Cylinder skirt	Comp. cylinder	Cone-ring
0.5	2.70	22	26	9	3	5
	3.16	31	32	22	5	7
	3.85	31	33	28	12	9
0.7	3.16	32	32	22	5	8
	3.85	30	32	27	12	9
	4.14	31	35	32	19	22
0.9	3.85	31	33	28	11	9
	4.14	31	35	30	18	22
	4.90	29	30	29	18	35
1.1	4.14	34	33	33	18	22
	4.90	30	31	30	19	35
1.3	4.90	30	29	30	19	35
	5.38	26	29	28	18	44

Table 4: Efficiency (%)-Displacement V=42.41m^3

The last examined configuration (figure 9) was subjected to a wave spectrum having H_s=1m and energy period varying in the range T_e=5~10 sec. Both the single body and the piston-like arrangement were examined. The PTO system was assumed to act either as linear damper or as the hydraulic system described previously.

The results for the efficiency (calculated on the basis of the wave energy corresponding to the width of the internal cylinder) and the absorbed power are shown in Table 5 and Figure 14 below.

Sea State		Floater			
H_s (m)	T_e (sec)	Single Cylinder Linear PTO	Single Cylinder Hydraulic PTO	Piston-like Linear PTO	Piston-Like Hydraulic PTO
1.0	5	58	48	100	83
	6	49	44	96	81
	7	39	37	70	65
	8	32	33	49	49
	9	25	29	40	39
	10	24	25	30	31

Table 5: Displacement V=117.8m^3 Absorption efficiency (%)

Considering the piston-like arrangement a serious increase in the absorbed power is depicted in the results, for periods near the 6 sec, which is close to the resonance frequency for the heave motion of the internal floater. Indicative extracts of the time histories of heave motion and instantaneous power absorption are shown in figures 12 and 13.

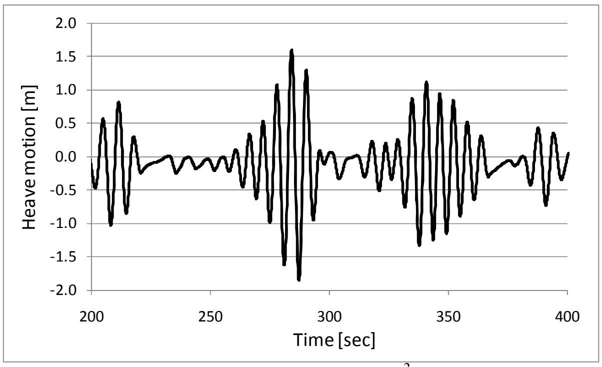

Figure 12: Displacement V=117.8m^3 Piston-Like & Hydraulic PTO, Heave motion Hs=1m, Te=6 sec.

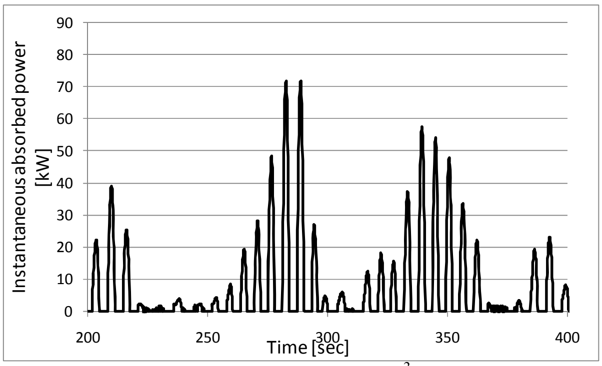

Figure 13: Displacement V=117.8m^3 Piston-Like & Hydraulic PTO, Inst. Power abs. Hs=1m, Te=6 sec.

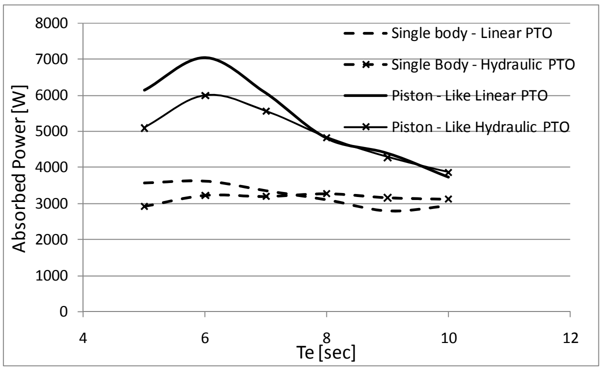

Figure 14: Single body and Piston-like arrangement comparison

6 Conclusions

A numerical model for the investigation of the effect that floaters' hydrodynamics has on the performance characteristics of tightly moored vertical axisymmetric wave energy converters was presented. The tightly moored wave energy converters were assumed to exploit their heave motion in producing useful power. The model included an exact formulation of the linear hydrodynamic properties of the floaters, including any interactions among the participating body components in concentric arrangements. The theoretical modeling of the mechanical components of the system was also described. A numerical scheme, suitable for the integration in the time domain of the non-linear equations of the motion was chosen. The influence of a range of the WEC parameters and incident wave spectra was examined. A considerable increase in the absorbed power was observed when the floater of the device was assumed to be surrounded by a concentric external torus.

Work is being currently under way to investigate in more details the non – linear phenomena that are associated with the exciting wave loads as well as with the hydraulic and PTO mechanism.

Acknowledgements

Authors wish to acknowledge the help of Mr Michael Apostolides in running the computer codes and preparing the graphs.

References

[1] Mavrakos, S.A., Katsaounis, G.M., Nielsen, K., Lemonis, G., 2004. "Numerical Performance Investigation of an Array of Heaving Wave Power Converters in Front of a Vertical Breakwater", *Proc. Int. Symp. on Offshore and Polar Engineering (ISOPE)* , Toulon, France.

[2] Mavrakos, S.A., Katsaounis, G.M., 2005. "Parametric Evaluation of the Performance Characteristics of Tightly Moored Wave Energy Converters". *Proc. 24th Int. Conf Offshore Mechanics and Arctic Engineering (OMAE)*, Halkidiki, Greece.

[3] Falnes, J., 2002. *Ocean Waves and Oscillating Systems*, Cambridge University Press.

[4] Eidsmoen, H., 1996. "Simulation of a Tight Moored Heqaving-Float Wave-Energy Converter". *Technical report, OWEC-1 project, Annex II, Float Systems*.

[5] Cummins, W.E., 1962. "The Impulse Response Function and Ship Motions", *Schiffstechnik*, 9.

[6] Faltinsen, O.M., 1990. *Sea Loads on Ships and Offshore Structures*, Cambridge University Press.

[7] Bathe, K.J., 1992. *Finite Element Procedures,* Prentice-Hall, New Jersey.

[8] Garrett, C.J.R., 1971. "Wave Forces on a Circular Dock", *Journal of Fluid Mechanics*, 46, pp. 129-139.

[9] Kokkinowrachos, K., Asorakos, S., Mavrakos, S. A.1980. *Belastungen und Bewegungen grossvolumiger Seebauwerke durch Wellen*, West-deutscher Verlag, Opladen, Germany.

[10] Kokkinowrachos, K., Mavrakos, S.A., Asorakos, S. 1986. "Behavior of Vertical Bodies of Revolution in Waves". *Ocean Engineering*, 13(6), pp. 505-538.

[11] Mavrakos, S.A., 1985. "Wave Loads on a Stationary Floating Bottomless Cylindrical Body with Finite Wall Thickness," *Applied Ocean Research*, **7**(4), pp. 213-224.

[12] Mavrakos, S.A., 2004. "Hydrodynamic Coefficients in Heave of Two Concentric Surface-Piercing Truncated Circular Cylinders", *Applied Ocean Research*, 26, pp. 84-97.

[13] Mavrakos, S.A. 2005. “Hydrodynamic characteristics of two concentric surface – piecing floating circular cylinders”, Proceedings, *11th International Maritime Association of the Mediterranean Conf.*, IMAM 2005, Lisboa, Portugal.